

1

1 **Data for the Reviewer#2 only:**

ng	Al	Ti	Mn	Fe	La	Ce	Nd	Date	Volume (L)
Insoluble									
Pluie 1 2010	162	25	4	166	0.08	0.17	0.07	24/11/10	0.536
Pluie 2 2010	893	134	17	746	0.56	1.26	0.47	26/11/10	0.041
Pluie 3 2010	84	22	3	129	0.07	0.17	0.07	30/11/10	0.453
Pluie 4 2010	1901	329	35	1719	1.05	2.70	0.96	30/11/10	0.210
Pluie 5 2010	543	133	12	628	0.26	0.76	0.24	06/12/10	0.538
Pluies 1_2 2005	347	77	14	398	0.22	0.54	0.19	30/01/05	0.460
Pluie 5 2005	5113	877	80	4526	2.68	6.58	2.43	12/02/05	0.550
Pluie 3 2008	111	24	2	109	0.06	0.12	0.04	07/12/08	0.320
Pluie 5 2008	240	58	4	270	0.10	0.26	0.09	09/12/08	0.317
Pluie 6 2008	25	7	1	55	0.02	0.07	0.01	10/12/08	0.101
Pluie 1 2009	26		1	37	0.02	0.04	0.01	05/12/09	0.324
Pluie 2 2009	897	143	14	713	0.41	1.19	0.35	07/12/09	0.085
Pluie 3 2009	179	27	3	164	0.12	0.30	0.10	11/12/09	0.030
Pluie 4 2009	36		1	45	0.03	0.07	0.02	15/12/09	0.104
Pluie 6 2009	90	12	2	113	0.07	0.17	0.07	28/12/09	0.538
Pluie 7 2009	232	31	4	242	0.10	0.50	0.08	03/01/10	0.333
Soluble									
Pluie 1 2010	381	12	33	216	0.39	0.92	0.25		
Pluie 2 2010	196	5	14	68	0.16	0.29	0.13		
Pluie 3 2010	2239	84	55	1244	1.79	4.70	1.86		
Pluie 4 2010	316	16	16	132	0.26	0.73	0.26		
Pluie 5 2010	775	25	63	380	0.99	2.00	0.83		
Pluies 1_2 2005	506	41	54	946	0.19	0.57	0.18		
Pluie 5 2005	179	9	21	295	0.20	0.42	0.13		
Pluie 3 2008	1309	77	13	481	1.06	2.05	0.75		
Pluie 5 2008	55	12	4	27	0.07	0.16	0.06		
Pluie 6 2008	488	37	9	320	0.46	0.85	0.35		
Pluie 1 2009	547	21	15	658	0.30	0.83	0.36		
Pluie 2 2009	43	2	3		0.02	0.04	0.00		
Pluie 3 2009	366	22	6	173	0.28	0.64	0.24		
Pluie 4 2009	364	12	11	136	0.33	0.72	0.31		
Pluie 6 2009	928	100	27	540	0.59	1.57	0.58		
Pluie 7 2009	101	8	6	7	0.05	0.19	0.02		
Blanks Soluble									
2010_BT1	250	13	1.8	167	0.02	0.04	0.02		0.12
2010_BT2	167	6	3.4	168	0.02	0.07	0.011		0.09
2010_BT3	55	2	0.4	10	0.004	0.02	0.005		0.07
2010_BT4	104	1	0.4	20	0.009	0.03			0.08
2010_BT5	39	1	0.2	7	0.004	0.02			0.04
2009_BLab1	18	6	0.7	13	0.005	0.06			0.10
2009_BLab2	52	4	1.9	127	0.010	0.08	0.009		0.10
2009_BLab3	17	4	0.4	8	0.009	0.06			0.10
2009_BLab4	21	8	0.5	65	0.009	0.06			0.10
2009_BT5	174	13	2.0	54	0.06	0.12	0.04		0.31
2009_BT16	89	3	1.6	104	0.011	0.18	0.007		0.09
Med	55	4	1	54	0.009	0.06	0.010		
MAD	55	3	1	68	0.006	0.03	0.015		
Moy	90	6	1	67	0.015	0.07	0.02		
Sig	77	4	1	64	0.02	0.05	0.013		
Blank InSoluble									
2010_BT1	41	17	0.2	25	0.002	0.02			
2010_BT2	40	14	0.3	25		0.01			
2010_BT3	40	9	0.2	21	0.010	0.03			
2010_BT4	41	9	0.2	22		0.00			
2010_BT5	58	16	0.3	22		0.01			
2009_BLab1	30	26	0.3	36	0.003	0.01			
2009_BLab2	31	19	0.2	28	0.002	0.02			
2009_BLab3	39	21	0.3	28	0.004	0.01			
2009_BLab4	42	16	0.5	28	0.010	0.03	0.01		
2009_BT5	40	22	0.3	21	0.003	0.02			
2009_BT16	27	19	0.3	31		0.01			
Med	40	17	0.3	25	0.003	0.015			
MAD	2	5	0.1	4	0.004	0.003			
Moy	39	17	0.3	26	0.005	0.015			
Sig	8	5	0.1	5	0.003	0.007			

3

3 **Supplementary reading for publication:**

4

Concentrations in µg/L	Rain volume (mL)	Al	Ti	Mn	Fe	La	Ce	Nd
Insoluble								
P1_10	536	0.30 ± 0.07	0.046 ± 0.026	0.0077 ± 0.0021	0.31 ± 0.06	0.00015 ± 0.00002	0.00033 ± 0.00006	0.00012 ± 0.00002
P3_10	453	0.19 ± 0.05	0.049 ± 0.029	0.0072 ± 0.0020	0.28 ± 0.06	0.00015 ± 0.00002	0.00038 ± 0.00007	0.00016 ± 0.00002
P3_08	320	0.35 ± 0.09	0.074 ± 0.043	0.0055 ± 0.0016	0.34 ± 0.07	0.00018 ± 0.00002	0.00039 ± 0.00007	0.00013 ± 0.00002
P6_08	101	0.25 ± 0.14	0.073 ± 0.091	0.011 ± 0.004	0.55 ± 0.14	0.00019 ± 0.00004	0.00073 ± 0.00016	0.000070 ± 0.000054
P3_09	30	6.0 ± 1.3	0.89 ± 0.49	0.11 ± 0.03	5.5 ± 1.1	0.0041 ± 0.0004	0.010 ± 0.002	0.0033 ± 0.0004
Soluble								
P1_10	536	0.71 ± 0.12	0.023 ± 0.007	0.061 ± 0.004	0.40 ± 0.13	0.00074 ± 0.00005	0.0017 ± 0.0002	0.00046 ± 0.00006
P3_10	453	4.9 ± 0.3	0.18 ± 0.02	0.12 ± 0.01	2.7 ± 0.2	0.0039 ± 0.0002	0.010 ± 0.001	0.0041 ± 0.0002
P3_08	320	4.1 ± 0.3	0.24 ± 0.03	0.042 ± 0.004	1.5 ± 0.2	0.0033 ± 0.0002	0.0064 ± 0.0007	0.0023 ± 0.0001
P6_08	101	4.8 ± 0.6	0.36 ± 0.06	0.089 ± 0.010	3.2 ± 0.7	0.0046 ± 0.0003	0.0084 ± 0.0010	0.0034 ± 0.0002
P3_09	30	12 ± 2	0.75 ± 0.16	0.21 ± 0.03	5.8 ± 2.3	0.0095 ± 0.0006	0.022 ± 0.003	0.0079 ± 0.0004

4

6 **Reviewed article (modification in yellow)**

7 **Solubility of iron and other trace elements in rainwater**
8 **collected on Kerguelen Islands (South Indian Ocean).**

9

10 **A. Heimbürger¹, R. Losno¹ and S. Triquet¹**

11 [1]{Laboratoire Interuniversitaire des Systèmes Atmosphériques, UMR CNRS 7583, Université
12 Paris Diderot, Université Paris Est-Créteil, F-94010 Créteil Cedex, France}

13 Correspondence to: A. Heimbürger (alexie.heimburger@lisa.u-pec.fr)

14

15 **Abstract**

16 The soluble fraction of aerosols that is deposited on the open ocean is vital for phytoplankton
17 growth. It is believed that a large proportion of this dissolved fraction is bioavailable for marine
18 biota and thus plays an important role in primary production, especially in HNLC oceanic areas
19 where this production is limited by micronutrient supply. There is still much uncertainty
20 surrounding the solubility of atmospheric particles in global biogeochemical cycles and it is not
21 well understood. In this study, we present the solubilities of seven elements (Al, Ce, Fe, La, Mn,
22 Nd, Ti) in rainwater on Kerguelen Islands, in the middle of the Southern Indian Ocean. The
23 solubilities of elements exhibit high values, generally greater than 70%, and Ti remains the least
24 soluble element. Because the Southern Indian Ocean is remote from its dust sources, only the
25 fraction of smaller aerosols reaches Kerguelen Islands after undergoing several cloud and chemical
26 processes during their transport resulting in a drastic increase in solubility. Finally, we deduced an
27 average soluble iron deposition flux of $27 \pm 6 \mu\text{g m}^{-2} \text{d}^{-1}$ ($\sim 0.5 \mu\text{mol m}^{-2} \text{d}^{-1}$) for the studied
28 oceanic area, taking into account a median iron solubility of $82\% \pm 18\%$.

29

30 **1 Introduction**

31 The Southern Ocean is known to be the largest High-Nitrate Low-Chlorophyll (HNLC) oceanic
32 area (de Baar et al., 1995). Such zones are characterized by a lack of micronutrients and trace

33 metals in surface waters limiting phytoplankton growth (Martin 1990; Boyd et al., 2000, 2007;
34 Blain et al., 2007). In HNLC area, primary production is especially limited by iron supply (Boyd et
35 al., 2007) and could be co-limited by other transition metals, such as manganese (Middag et al.,
36 2011), copper (Annett et al., 2008), cobalt (Saito et al., 2002), zinc (Morel et al., 1991) and nickel
37 (Price and Morel, 1991). Atmospheric deposition is recognized to play an essential role in
38 biogeochemical cycles in remote ocean areas (Duce and Tindale, 1991; Fung et al., 2000; Jickells et
39 al., 2005), even at extremely low levels (Morel and Price, 2003): it brings new external trace metals
40 into surface waters and thus vital bioavailable nutrients for marine biota. It is often assumed that the
41 dissolved forms of trace metals in atmospheric deposition are directly available for phytoplankton
42 because bioavailability is difficult to measure (e. g. Shi et al. [2012]). Indeed, bioavailability
43 depends on several factors, which have to be taken into account to determine it, such as the
44 presence of others nutrients in euphotic surface waters, the residence time of deposited atmospheric
45 particles in surface waters, the soluble fraction and the physicochemical speciation of trace metals
46 in seawater (Boyd, 2002; Boyd et al., 2010). Even if phytoplankton only uses a fraction of
47 atmospheric soluble trace metals in its metabolism (Visser et al., 2003), the best proxy so far is
48 taking the soluble fraction of metals as the bioavailable part of these metals for marine biota (Shi et
49 al., 2012). This dissolved fraction expressed as percentage is referred to as “solubility”, for which
50 definition depends on the considered science field (e. g. oceanographic and atmospheric sciences)
51 and the usage context. In this paper, we will define solubility in section 3.1. Numerous studies have
52 been carried out on iron solubility and its controlling factors. Soluble iron in soil represents 0.5% of
53 the total iron (Hand et al., 2004) while it ranges from 0.1% to 90% in aerosols, rains and snows,
54 sampled at different places and times (e.g., Losno 1989; Colin et al., 1990; Zhuang et al., 1992;
55 Guieu et al., 1997; Edwards and Sedwick, 2001; Kieber et al., 2003; Chen and Siefert, 2004; Baker
56 et al., 2006; Buck et al., 2010b; Theodosi et al., 2010; Witt et al., 2010). Most of the solubility
57 values for atmospheric samples are summarized in Mahowald et al. (2005) and Fan et al. (2006).
58 Variability of iron solubility in the atmosphere is controlled by interactions such as photochemical
59 reactions, cloud processes and organic complexation (e.g., Losno 1989; Zhuang et al., 1992; Kieber
60 et al., 2003; Hand et al., 2004; Chen and Siefert, 2004; Desboeufs et al., 2001, 2005; Paris et al.,
61 2011), as well as mineralogy of dust sources (Journet et al., 2008) and the element's enrichment
62 factor relative to its natural crustal abundance. Baker and Jickells (2006) also suggested that dust
63 iron solubility may instead be controlled by particle size but this hypothesis was contradicted in
64 Buck et al. (2010a) and Paris et al. (2010). All of these factors combined together can explain the

65 wide range of iron solubility values found in the literature. But, it has to be noted here that part of
66 this range is also due to different experimental protocols used by different researchers for
67 investigating the solubility, which hinder our understanding of the factors controlling solubility (e.
68 g. Baker and Croot, 2010; Witt et al., 2010; Shi et al., 2012 ; Buck and Paytan, 2012 ; Morton et al.,
69 2013). Other studies have observed that the soluble part of other trace elements is highly variable
70 and heterogeneous too. For example, reported solubility ranges from 0.1% to 90% for aluminium
71 and from 10% to 100% for manganese (e.g., Jickells et al., 1992; Colin et al., 1990; Losno et al.,
72 1993; Lim et al., 1994; Guieu et al., 1997; Desboeufs et al., 2005; Baker et al., 2006; Buck et al.,
73 2010b; Hsu et al., 2010; Theodosi et al., 2010; Witt et al., 2010).

74 Compared to the North Hemisphere, atmospheric supply of micronutrients is believed to be small
75 over the Southern Ocean (Fung et al., 2000; Prospero et al., 2002; Jickells et al., 2005; Mahowald et
76 al., 2005) due to its remote distance from dust sources. In a previous paper, Heimbürger et al.
77 (2012a) demonstrated that atmospheric inputs have to be re-evaluated in the Indian part of the
78 Southern Ocean: the authors found that direct measured dust flux is 20 times higher than the
79 previous estimation calculated by Wagener et al. (2008). Therefore, it is highly probable that
80 variation of atmospheric deposition in such an area may strongly influence marine biology and thus
81 carbon sequestration since the Southern Ocean is depicted as the largest potential sink of
82 anthropogenic CO₂ in the global ocean (Sarmiento et al., 1998; Caldeira and Duffy, 2000; Schlitzer,
83 2000). In this paper, we present measurements of soluble and insoluble composition for crustal
84 elements, including iron, in rainwater samples collected on Kerguelen Islands in the Southern
85 Indian Ocean. To our knowledge up to now such measurements have never been taken over this
86 oceanic region.

87

88 **2 Materials and methods**

89 **2.1 Sampling site**

90 The studied area was located on Kerguelen Archipelago (48°35'S - 49°54'S; 68°43'E – 70°35'E), in
91 the Southern Indian Ocean, approximately 3800 km south-east of South Africa and 2000 km from
92 the Antarctic coast (Fig 1a). Rain sampling was carried out during four summer campaigns, one
93 under the program KEFREN (“Kerguelen : Erosion and Fallout of tRace Elements and Nitrogen”)
94 and three under the FLATOCOA one (“Flux Atmosphérique d'Origine Continentale de l'Océan
95 Austral”). Both programs were supported by IPEV (“Institut polaire française Paul Emile Victor”).

96 A total of 14 single rain events were collected; they are divided as follows: *i*) two rains were
97 collected from 30 January to 13 February 2005 (named P1/2_05 and P5_05), *ii*) three rains from 3
98 to 11 December 2008 (P3_08, P5_08, P6_08), *iii*) four rains from 5 December 2009 to 4 January
99 2010 (P2_09, P3_09, P6_09, P7_09) and *iv*) five rains from 24 November to 11 December 2010
100 (from P1_10 to P5_10). The sampling site (49°21'10.3" S, 70°12'58.3" E) was installed near the
101 chapel *Notre Dame des Vents*, north-west of the only permanently-occupied base of the archipelago
102 *Port-aux-Français* (PAF) (Fig. 1b).

103

104 2.2 Materials

105 Rains were sampled using a collector placed on top of a 100 mm diameter and 2 m high vertically
106 erected PVC pipe (Fig. 2a). This collector is made from a 24 cm diameter low density polyethylene
107 (PE) funnel attached to an on-line filtration device (Fig. 2b). The filtration device is composed of
108 several parts: a machined high density PE cable fitting holds the bottom end of the funnel and
109 supports a Teflon[®] filter holder equipped with a clipped Nuclepore[®] polycarbonate membrane (PC)
110 filter (porosity : 0.2 µm, diameter : 47 mm) on a PC supporting grid. The filter holder is placed on
111 the top of a 30 cm high closed section of tubing that is fitted to a 500 mL polypropylene (PP) bottle.
112 A small Teflon[®] pipe lets filtered water flow freely into the bottle. The insoluble fraction of
113 rainwater remains on the surface of the PC filter while the soluble fraction flows by gravity into the
114 PP bottle (Nalgene[®]). The only pieces of equipment that touch the rainwater are the funnel, the
115 Teflon[®] filter holder, the PC filters, the PC filter supporting grid and the PP bottles (Fig. 2b).

116 All the sampling materials were thoroughly washed in the laboratory before the campaign. The
117 500 mL PP bottles and Teflon[®] parts underwent the same washing protocol as described in
118 Heimburger et al. (2012a) for total deposition devices. All of the other materials were: *i*) washed
119 using ordinary dish detergent in an ISO 8 controlled laboratory room, *ii*) soaked from two days to
120 one week in a bath of 2% Decon[®] detergent diluted with reverse-osmosed water (purified water) and
121 *iii*) soaked from two to three weeks in 2% v/v Normapur[®] analytic grade hydrochloric acid.
122 Extensive rinsing was performed between each step with reverse-osmosed water. Materials were
123 then transferred to an ISO 5 clean room and: *iv*) rinsed in ElgaTM Purelab ultra[®] pure water and
124 *v*) soaked in a high purity hydrochloric acid solution (2% MerkTM Suprapur[®]), except for the
125 funnels, which were too large for our soaking baths. In an ISO 1 laminar flow bench, these
126 materials were finally: *vi*) rinsed once (three times for the funnels) with 2% high purity

127 hydrochloric acid solution, *vii*) five times with ultra pure water and *viii*) left until dry (two to four
128 hours). Once all the materials had been washed and dried, the funnels were mounted on their high
129 density PE cable fittings under the ISO 1 laminar flow bench and the last three steps of the washing
130 protocol were repeated. They were then individually placed in bags that had been washed in the
131 same way as the materials, and were stored until being used only once in the field. The Nuclepore®
132 PC filters (0.2 µm porosity, diameter : 47 mm) were *i*) washed in a bath of 2 % v/v Romil-UpA™
133 HCl for almost 2 h under the ISO 1 laminar flow bench, then *ii*) rinsed with ultra pure water, *iii*)
134 clipped with special rings (FilClip®), previously washed by the protocol for materials described
135 above, and *iv*) stored individually in washed polystyrene Petri dishes until use.

136

137 2.3 Rain sampling

138 A clean hood (AirC2, ISO 2 quality), which provided an ultra-clean work zone, was installed inside
139 a dedicated clean area (ISO 6-ISO 7 quality) in the PAF scientific building (see Heimbürger et al.
140 (2012a) for more details). It allowed us to prepare rain devices before sampling: *i*) a clipped filter
141 was placed in the Teflon® filter holder, *ii*) a 500 mL PP bottle without its cork was introduced into
142 the 30 cm high closed tubing (the cork was stored in a clean box intended for this purpose) and *iii*) a
143 funnel with its cable fitting + Teflon® filter holder were screwed on to the top of the closed tubing.
144 The plastic bag protecting the funnel's aperture had to be kept in place; a crack was made at the
145 level of the cable fitting.

146 The sampling started at the beginning of a rain event. A prepared rain device was placed on the top
147 of the PVC pipe; the plastic bag protecting the funnel was removed and conserved. Once the rain
148 event had finished, the funnel was covered by its plastic bag and the device was brought into the
149 clean hood in the scientific building. A vacuum was applied to the section of tubing to help the last
150 rain drops to pass through the filter. The funnel was then removed and no longer used (a new one
151 was used for each sampling). The clipped filter was stored in a clean Petri dish and the 500 mL
152 bottle was weighed. Finally, less than half an hour after the collection of the sample, part of the
153 soluble fraction of rain was stored in a 60 mL Teflon® bottle. Teflon® bottles have undergone the
154 same washing protocol as the 500 mL bottles. They contained enough Romil-UpA™ HNO₃ to give a
155 1% concentration of acid when filled with the collected rain ; the acid solution was used to prevent
156 adsorption of trace metals into the Teflon® bottle walls during the storage of samples (between six
157 months and two years) before trace metal analyses back in the laboratory. During the 2008

158 campaign, the pH of samples was immediately measured after sampling: it is equal to 5.4 ± 0.2
159 (mean $\pm \sigma$, σ = standard deviation) for all the samples. The Teflon[®] filter holder was then rinsed
160 once with 2% *MerkTM Suprapur[®]* hydrochloric acid solution, five times with ultra pure water and
161 allowed to dry in the clean hood before being used for the next sampling. Four laboratory blanks
162 and eight field blanks were performed by simulating a rain event with *ElgaTM Purelab ultra[®]* pure
163 water in an ISO 5 clean room and in the field respectively.

164

165 2.4 Sample preparation and analyses

166 Back in the laboratory and just before analyses, the soluble fractions of rains (stored in 60 mL 1%
167 HNO₃ acidified Teflon[®] bottles) were transferred into PP 15 mL sample vials that had been
168 thoroughly washed (see Heimburger et al. (2012a) for details of the washing protocol). The contents
169 of vials were analysed using High Resolution – Inductively Coupled Plasma – Mass Spectrometry
170 (HR-ICP-MS, *Thermo Fisher ScientificTM Element 2*), which was installed in an ISO 5 clean room
171 and calibrated by diluted acidified multi-element external standards. The sample introduction
172 system was protected by an ISO 1 box.

173 The contours of the clipped filters, which contained the insoluble fractions of rains, were cut using a
174 new clean stainless steel scalpel blade. The filters of rain samples, laboratory blanks and field
175 blanks were then digested using 4 mL of a HNO₃ / H₂O / HF solution (proportion: 3 / 1 / 0.5 of pure
176 *Romil-UpATM HNO₃* / ultra pure water / *MerkTM Ultrapur[®] HF*) during 14 h in an air oven at 130°C
177 in closed SavillexTM PFA digestion vessels. Vessels had undergone the same washing protocol as
178 described in Heimburger et al. (2012a) followed by a trial digestion. These vessels were then rinsed
179 and filled with 2% *Romil-UpATM HCl* until being used. At the end of digestion, the HF was
180 completely evaporated on a heater plate. 5 mL of 1% *Romil-UpATM HNO₃* plus 0.5 mL of *Romil-*
181 *UpATM H₂O₂* were then added and left on the plate for 30 minutes. Finally, the content of each vessel
182 was transferred into a 60 mL PP bottle (same washing protocol as for the bottles containing rain
183 samples) with the 1% *Romil-UpATM HNO₃* solution used to rinse the vessel walls. These samples
184 were then analyzed by HR-ICP-MS as well. Seven blank Nuclepore[®] PC filters underwent the
185 digestion protocol in order to estimate possible contamination from the filters and the digestion
186 experiments. 6 mg of BE-N (*Basalt from SARM laboratory, France*) and 8.6 mg of SDC-1 (*Mica*
187 *Schist from USGS, USA*) geostandards, crushed prior to use, also underwent this protocol in order
188 to estimate the yield and accuracy of our digestion method.

189 Analytical blanks (n = 7) were carried out using 1% v/v *Romil-UpA*TM HNO₃ in order to determine
 190 the analytical detection limits (DL) of the HR-ICP-MS method. The accuracy (expressed as
 191 recovery rate: RR% = mean of measured standard concentrations / certified or published values)
 192 and reproducibility (expressed as relative standard deviation: RSD% = σ / mean) of measurements
 193 were checked using the certified reference material (CRM) SLRS-5 (Heimburger et al., 2012b)
 194 commonly used to control trace metals analysis. This CRM was diluted ten times using 1% v/v
 195 *Romil-UpA*TM ultra-pure nitric acid in ultra-pure water in order to find more similar concentrations
 196 between the SLRS-5 and the ones found in samples, allowing calculation of significant RR% and
 197 RSD% (Feinberg, 2009). Table 1 presents DL, RSD% and RR% for a set of analysed elements, for
 198 which results were validated (see section 3.1) and so discussed afterwards. All the measured
 199 concentrations including blanks were above DL: they are three times higher than DL in samples,
 200 except for Nd for the soluble fraction. Reproducibility of SLRS-5 measurements is under or equal to
 201 10% for all the elements; accuracy is between 94% and 109%. Measured concentrations in BE-N
 202 and SDC-1 geostandards are fairly consistent with the certified ones: RR% are generally equal to
 203 100% \pm 30% .

204

205 3 Results and discussion

206 3.1 Solubility uncertainties

207 The solubility in rainwater is expressed as follows:

$$208 \quad S_X \% = \frac{[X]_{soluble}}{[X]_{total}} \quad (1)$$

209 where S_X % is the solubility of an element X, $[X]_{soluble}$ is the soluble concentration of X, $[X]_{insoluble}$ is
 210 the insoluble concentration of X and $[X]_{total}$ is the sum of $[X]_{soluble}$ and $[X]_{insoluble}$. The soluble
 211 fraction is defined here as the amount of metals in rainwater which passes through the 0,2 μ m PC
 212 membrane filter. The insoluble one is defined as the amount which stay on the PC filter. If we
 213 assume that rainwater is aerosol particles trapped in water drops, solubility is then defined as the
 214 fraction of metals that is dissolved in rainwater (i. e. the metal content in the filtrated rain divided
 215 by the total metal content in rain) (e.g. Lim et al., 1994; Buck et al., 2010b). This solubility is related
 216 to the "fractional solubility" defined by Baker and Croot (2010) for laboratory experiments on
 217 aerosol dissolution. Filtration of rainwater during the sampling provides a direct measurement of

218 natural solubility.

219 To determine $[X]_{soluble}$ and $[X]_{insoluble}$, we took into account the contamination observed in the
 220 different blanks performed (laboratory blanks, field blanks, blank filters; see Sect. 2.) for both
 221 soluble and insoluble fractions respectively. This contamination is caused by elements remaining in
 222 sampling devices, including filters and the walls of equipment in contact with samples. For a given
 223 element X, we computed its quantities (Q_i) in each blank by multiplying measured blank
 224 concentrations by blank volumes. For the elements presented in this paper, these quantities are
 225 found to be similar for both laboratory and field blanks; the quantities in filter blanks are also
 226 equivalent to the ones in laboratory and field insoluble blanks. Therefore, all the blanks were pooled
 227 together for both fractions respectively in order to extract a global blank defined as the median
 228 quantity of all the blank quantities. Figure 3 represents ratios of this median quantity in blanks
 229 relative to the one in rainwater, for all the analysed elements in the soluble and insoluble fractions
 230 respectively. Expressed as a percentage, these ratios are under 10 % for Ce, La, Mn and Nd for both
 231 fractions, under 20% for Al and Fe for both fractions, and reach 35% for Ti for the insoluble
 232 fraction only. It has to be noted here that other elements (Co, Cr, Cu, Ni, V, Pb, Zn) were also
 233 analysed in rainwater but their ratio values (median quantity in blanks relative to the one in
 234 rainwater) were higher than 40 % for the both soluble and insoluble fractions, and even equal to
 235 100 % for Ni and Cu. Thanks to all the blanks we performed, this contamination was identified as
 236 coming from PC filters. Although careful washing of these filters, filter blanks exhibit high
 237 quantities of Co, Cu, Cr, Ni, V, Pb and Zn compared to the median quantities found in rain samples
 238 for these elements after blank corrections. It leads to a contamination of the soluble fraction of
 239 laboratory and field blanks, for which no other significant contamination were observed.

240 For the validated elements (Al, Ce, Fe, La, Mn, Nd, Ti), the median quantity in blanks was
 241 subtracted from the ones found in rain samples for each element. $[X]_{soluble}$ and $[X]_{insoluble}$ are
 242 consequently given by the following formulas:

$$243 \quad [X]_{soluble} = \frac{[X]_{analytical} V_{rain} - median(Q_i)}{V_{rain}} \quad (2)$$

$$244 \quad [X]_{insoluble} = \frac{[X]_{analytical} V_{insoluble} - median(Q_i)}{V_{rain}} \quad (3)$$

245 where $[X]_{analytical}$ represents measured concentrations, V_{rain} the volumes of collected rainwater, and
 246 $V_{insoluble}$ the dilution volumes of the digested insoluble fraction. Uncertainties associated with

247 $[X]_{\text{analytical}}$ ($\sigma([X]_{\text{analytical}})$) are computed using standard deviations and the mathematical approach of
 248 exact differential (Feinberg, 2009). Because the quantities of all the blanks are not normally
 249 distributed, we used robust statistics for a better estimation of the blank distribution range (Feinberg
 250 2009).

$$251 \quad \sigma([X]_{\text{analytical}}) = \sqrt{DL^2 + ([X]_{\text{analytical}} RSD\%)^2 + ([X]_{\text{analytical}} (1 - RR\%))^2} \quad (4)$$

252 where $(1 - RR\%)$ is the accuracy error from SLRS-5 measurements. Standard deviations of $[X]_{\text{soluble}}$
 253 and $[X]_{\text{insoluble}}$ are then computed as follows:

$$254 \quad \sigma([X]_{\text{soluble}}) = \frac{\sqrt{(\sigma[X]_{\text{analytical}} V_{\text{rain}})^2 + (1.483 MAD)^2}}{V_{\text{rain}}} \quad (5)$$

$$255 \quad \sigma([X]_{\text{insoluble}}) = \frac{\sqrt{(\sigma[X]_{\text{analytical}} V_{\text{insoluble}})^2 + (1.483 MAD)^2}}{V_{\text{rain}}} \quad (6)$$

256 with median absolute deviation $MAD = \text{median}(|Q_i - \text{median}(Q_i)|)$ representing the dispersion of
 257 blank distribution. Finally, solubility uncertainties are given by the Eq. (7):

$$258 \quad \Delta S_X \% = k S_X \% \frac{[X]_{\text{insoluble}}}{[X]_{\text{soluble}}} \sqrt{\frac{\left(\frac{\sigma[X]_{\text{soluble}}}{[X]_{\text{soluble}}}\right)^2 + \left(\frac{\sigma[X]_{\text{insoluble}}}{[X]_{\text{insoluble}}}\right)^2}{1 + \frac{[X]_{\text{insoluble}}}{[X]_{\text{soluble}}}}} \quad (7)$$

259 with the coverage factor of $k = 2$ (Feinberg, 2009), which allows us to obtain an expanded
 260 uncertainty representing a confidence level of 95%, i.e. this expanded uncertainty includes 95% of
 261 possible solubility values.

262

263 3.2. Local contamination issues

264 Rain samples may be contaminated by local soil emission due to human activities on PAF occurring
 265 not far enough from the sampling site: soil portions are occasionally moved because of track
 266 maintenance generating exposed surfaces that produce local emission spots. Heimburger et al.
 267 (2012a) demonstrated that Ti/Al ratio is a suitable tracer for such contamination: the authors
 268 reported that these ratios are equal to 0.15 ± 0.05 (mean $\pm \sigma$) and 0.04 ± 0.01 in soil and
 269 atmospheric deposition samples respectively. Consequently, the $[Ti]_{\text{total}}/[Al]_{\text{total}}$ ratio was computed

270 for each rain sample (Fig. 4). Uncertainty on this ratio was computed by the following formulas:

$$271 \quad \sigma\left(\frac{[Ti]_{total}}{[Al]_{total}}\right) = (Ti/Al) \sqrt{\left(\frac{\sigma[Ti]_{total}}{[Ti]_{total}}\right)^2 + \left(\frac{\sigma[Al]_{total}}{[Al]_{total}}\right)^2} \quad (8)$$

272 with

$$273 \quad \sigma([X]_{total}) = \sqrt{\sigma[X]_{insoluble}^2 + \sigma[X]_{soluble}^2} \quad (9)$$

274 Rains from P6_09 to P5_08 on Fig. 4 present Ti/Al ratios consistent with the one found in
 275 Kerguelen's soil, which is not compatible with pure long range transported particles, and so they
 276 were not discussed afterwards. Rain P3_10 exhibits a Ti/Al ratio incompatible with local soil
 277 contamination and in the range found in deposition samples (Heimbürger et al., 2012a). Four rains
 278 (P1_10, P3_08, P6_08, P3_09) have a Ti/Al ratio between the ones in soils and in deposition. If we
 279 take into account standard deviation calculated with the Eq. 8 and Eq. 9, a local soil contamination
 280 is less probable for P1_10 and P3_08 than for P6_08 and P3_09, for which a small recovery of
 281 ranges of both soils and samples is observed. Nevertheless no strong discriminating criterion was
 282 found for these four rains, they will be included with rain P3_10 in the following discussion
 283 (insoluble and soluble concentrations of these five selected rains are available in supplementary
 284 reading).

285 To insure that no other local contamination from anthropogenic activities taking place on PAF, we
 286 used gdas re-analyzed archives (Draxler and Rolph, 2012; Rolph, 2012) to observe wind direction
 287 during the respective sampling times of the five kept rains. The base PAF is located East of the
 288 sampling site. For the five rains, winds came from opposite sectors of PAF, excluding wind
 289 transported contamination from the base (Table 2).

290

291 3.3. Rain event fluxes

292 Deposition fluxes generated by single rain events were computed by dividing the quantities found in
 293 each validated rain sample by the surface of the funnel aperture (0.045 m²). In Heimbürger et al.
 294 (2013), the authors found that atmospheric total deposition fluxes for the oceanic area of Kerguelen
 295 and Crozet Islands, averaged over 2009-2010, are equal to $53 \pm 2 \mu\text{g m}^{-2} \text{d}^{-1}$ and $33 \pm 1 \mu\text{g m}^{-2} \text{d}^{-1}$
 296 for Al and Fe respectively. Here, we found averaged rain fluxes (wet fluxes) equal to (mean $\pm \sigma$)
 297 $24 \pm 18 \mu\text{g m}^{-2}$ per rain events for Al and $14 \pm 10 \mu\text{g m}^{-2}$ per rain events for Fe (Table 3). Because
 298 dust deposition is controlled by wet deposition on Kerguelen Islands (Heimbürger et al., 2012a), we
 299 can neglect the dry deposition flux and thus we can assimilate total deposition flux to the wet

300 deposition one (rainwater events). Taking into account meteorological data that we recorded 8 km
301 from PAF, rain events occur from once a day to every two days, and so with a frequency of 0.5 to 1
302 per day. Applying this frequency on deposition flux values from Heimburger et al. (2013), the
303 averaged deposition flux on Kerguelen Islands is 51 to 110 $\mu\text{g m}^{-2}$ per rain event for Al and 32 to
304 68 $\mu\text{g m}^{-2}$ per rain event for Fe. These flux values are higher than the ones found in rainwater but
305 they have the same order of magnitude. We can then conclude that rain samples studied in this
306 paper are not unusual events.

307

308 3.4. Solubility

309 Before this study, no observed solubility values in rainwater were available in the literature for the
310 oceanic area of Kerguelen Islands. Our values can help to better quantify and model (chemistry and
311 transport) the part of atmospheric iron, which can be bioavailable for phytoplankton in the Southern
312 Indian Ocean. Solubilities in rains are reported in Table 4: they are higher than 70% for all the
313 elements (Al, Ce, Fe, La, Mn, Nd, Ti) for the five considered rain, except for Ti ($33\% \pm 44\%$ and
314 $46\% \pm 32\%$) and Fe ($57\% \pm 17\%$ and $51\% \pm 22\%$) in P1_10 and P3_09 respectively. The rare
315 earth elements (La, Ce and Nd) also exhibit high solubility values ranging from 68% to 98%. In
316 contrast, solubilities measured for the rejected rain samples show much lower values, for example
317 with a median of 17% for Ti, 9% for Fe and 30% for Al. High solubilities were already observed for
318 some of these elements in the literature. Siefert et al (1999) wrote that "labile Fe" solubility in the
319 fine dust fraction is more than 80% in aerosols collected on-board, while Edwards and Sedwick
320 (2001) reported a Fe solubility ranging from 9% to 89% in snow samples collected in Antarctica
321 and Baker and Croot (2010) modelled a Fe solubility between 0.2% and 100% over the Southern
322 Indian Ocean. Witt et al. (2010) found that Al solubility can reach $91\% \pm 66\%$ when the soluble
323 fraction of aerosols collected in the North Indian Ocean was extracted with a pH 1 solution. Mn
324 solubility can reach more than 90% in oceanic areas (Baker et al., 2006) and is known to be highly
325 variable (Losno, 1989; Desboeufs et al., 2005; Buck et al., 2010b). Nonetheless, Ti solubility
326 generally exhibits a lower value ($<15\%$) (Buck et al., 2010b; Hsu et al., 2010) than the ones found
327 on Kerguelen Islands (median = $76\% \pm 13\%$) although Ti remains the least soluble element in our
328 samples. We did not find any previously published solubility values for La, Ce or Nd. High
329 solubility of Ti informs us that dissolution processes in the atmosphere are very efficient and
330 probably destroy all the solid phases forming original aerosols, including the ones containing REE.

331 Several studies demonstrate that aerosol solubility increases during particle transport, especially due
332 to cloud processes (Zhuang et al., 1992; Gieray et al., 1997; Desboeufs et al., 2001). It is believed
333 that during their transport in the atmosphere aerosols typically undergo around 10
334 condensation/evaporation cloud cycles (Pruppacher and Jaenicke, 1995). In clouds, trace gases,
335 such as HNO₃, SO₂ and NH₃, are present and modify the pH of cloud droplets, which can increase
336 the soluble fraction of mineral particles. Organic molecules can also increase solubility, e.g. oxalate
337 complexation promoting iron solubility (Paris et al., 2011), as well as photochemistry processes, as
338 reviewed in Shi et al. (2012). Moreover, the average size of mineral aerosols decreases with
339 distance from dust sources, as a result of higher deposition rates for larger particles (Duce et al.,
340 1991). When mineral aerosol size becomes smaller, a greater proportion of their volume is exposed
341 to surface processes (Baker and Jickells, 2006) and is therefore available for dissolution. Ito (2012)
342 support the hypothesis that smaller dust particles yield increased iron solubility relative to larger
343 particles as a result of acid mobilization in smaller particles. In consequence, the smaller the
344 aerosols are and the further they are from their source area, the more soluble they are (Baker and
345 Jickells, 2006). Taking into account both of these hypotheses, we can explain the high solubilities
346 observed on Kerguelen Islands by long range transport from dust sources, which have been
347 identified as South America, South Africa and/or Australia (Prospero et al., 2002; Mahowald et al.,
348 2007; Bhattachan et al., 2012). Indeed, Wagener et al. (2008) and Heimbürger et al. (2012a) noted
349 that particles observed on Kerguelen Islands at sea or ground level exhibit 2 µm median diameters,
350 suggesting that only the fine dust fraction, which is believed to be more soluble than the larger dust
351 fraction, reaches Kerguelen Islands. In addition, air mass back trajectories computed from a Hybrid
352 Single Particle Lagrangian Integrated trajectory from the NOAA Air Resource Laboratory
353 (HYSPLIT) model (Draxler and Rolph, 2012; Rolph, 2012) with re-analysed archived
354 meteorological data (gdas) show that air masses travelled for at least five days over the ocean before
355 arriving at our sampling location during the five rain collection period. These air masses did not
356 pass over continents and so did not gain new less soluble continental aerosols. In consequence,
357 continental aerosols coming to Kerguelen Islands underwent several cloud processes during their
358 long range transport in the atmosphere and over the ocean, which probably dramatically increased
359 their solubilities.

361 **4 Conclusion**

362 Out of a total of 14 single rain events collected on Kerguelen Islands, five samples considered as
363 free of local contamination were validated and are representative of long range transported particles
364 deposited by rain events. Soluble and insoluble fractions of rainwater were immediately separated
365 during sampling allowing chemical evolution of some elements, such as Fe, to be kept to a
366 minimum. We found very high solubilities ($> 70\%$) for all the analysed elements, even the rare earth
367 elements, for which these are the first solubility values to be measured in an oceanic area, to our
368 knowledge. Consistently, Ti remains the least soluble element and we can suppose that other
369 elements and of importance in biogeochemical cycles, such as Co, Ni and Cu, have solubilities at
370 least equal to the solubility value of Ti (median $\pm \sigma = 63\% \pm 23\%$). Heimbürger et al. (2013)
371 reported an iron deposition flux of $33 \pm 1 \mu\text{g m}^{-2} \text{d}^{-1}$ on Kerguelen Islands. Applying the median
372 ($\pm \sigma$) iron solubility of $82\% \pm 18\%$ (Table 4), the deduced soluble iron flux is equal to
373 $27 \pm 6 \mu\text{g m}^{-2} \text{d}^{-1}$ for this oceanic area. This value is three times higher than the dissolved iron flux
374 in the Southern Indian Ocean according to the model proposed by Fan et al. (2006) taking into
375 account solubility processes with a 17% average solubility calculated for modelled wet deposition,
376 the predominant atmospheric deposition type on Kerguelen Islands (Heimbürger et al., 2012a). To
377 conclude, this experiment produced results for three validated samples only but strongly suggests
378 that solubility processes should be re-evaluated, as should soluble depositions simulated by current
379 atmospheric models for remote oceanic areas such as the Southern Ocean.

380

381 **Acknowledgements**

382 We would like to thank the *Institut polaire Paul Emile Victor* (IPEV), which provided funding and
383 enabled us to run KEFREN and FLATOCOA programs. We also thank the *Terres Australes et*
384 *Antarctiques Françaises* (TAAF) team and Elisabeth Bon Nguyen for their help. The authors
385 gratefully acknowledge the NOAA Air Resources Laboratory (ARL) for the provision of the
386 HYSPLIT transport and dispersion model and/or READY website (<http://ready.arl.noaa.gov>) used
387 in this publication.

388 **References**

- 389 Annett, A. L., Lapi, S., Ruth, T.J., and Maldonado, M.T.: The effects of Cu and Fe availability on
 390 the growth and Cu:C ratios of marine diatoms, *Limnol. Oceanogr.*, 53(6), 2451-2461, doi:
 391 10.4319/lo.2008.53.6.2451, 2008.
- 392 de Baar, H. J. W., de Jong, J. T. M., Bakker, D. C. E., Loscher, B. M., Veth, C., Bathmann, U., and
 393 Smetacek, V.: Importance of iron for plankton blooms and carbon dioxide drawdown in the
 394 Southern Ocean, *Nature*, 373 (6513), 412-415, doi: 10.1038/373412a0, 1995.
- 395 Baker, A. R., and Jickells, T. D.: Mineral particle size as a control on aerosol iron solubility,
 396 *Geophys. Res. Lett.*, 33, L17608, doi: 10.1029/2006GL026557, 2006.
- 397 Baker, A. R., Jickells, T. D., Witt, M., and Linge, K. L.: Trend in the solubility of iron, aluminium,
 398 manganese and phosphorus in aerosol collected over the Atlantic Ocean, *Mar. Chem.*, 98, 43-58,
 399 doi: 10.1016/j.marchem.2005.06.004, 2006.
- 400 Baker, A. R., and Croot, P. L.: Atmospheric and marine controls on aerosol iron solubility in
 401 seawater, *Mar. Chem.*, 120, 4-13, doi:10.1016/j.marchem.2008.09.003, 2010.
- 402 Bhattachan, A., D'Odorico, P., Baddock, M. C., Zobeck, T. M., Okin, G. S., and Cassar, N. : The
 403 Southern Kalahari: a potential new dust source in the Southern Hemisphere?, *Environ. Res. Lett.*, 7,
 404 7pp, doi:10.1088/1748-9326/7/2/024001, 2012.
- 405 Blain, S., Quéguiner, B., Armand, L., Belviso, S., Bombled, B., Bopp, L., Bowie, A., Brunet, C.,
 406 Brussard, C., Carlotti, F., Christaki, U., Corbière, A., Durand, I., Ebersbach, F., Fuda, J-L., Garcia,
 407 N., Gerringa, L., Griffiths, B., Guigue, C., Guillerm, C., Jacquet, S., Jeandel, C., Laan, P., Lefèvre,
 408 D., Monaco, C. L., Malits, A., Mosseri, J., Obernosterer, I., Park, Y.-H., Picheral, M., Pondaven, P.,
 409 Remenyi, T., Sandroni, V., Sarthou, G., Savoye, N., Scouarnec, L., Souhaut, M., Thuiller, D.,
 410 Timmermans, K., Trull, T., Uitz, J., van Beek, P., Veldhuis, M., Vincent, D., Viollier, E., Vong, L., T.
 411 Wagener T.: Effect of natural iron fertilization on carbon sequestration in the Southern Ocean,
 412 *Nature*, 446, 1070-1074, doi :10.1038/nature05700, 2007.
- 413 Boyd, P. W., Watson, A. J., Law, C. S., Abraham, E. R., Trull, T., Murdoch, R., Bakker, D. C.,
 414 Bowie, A. R., Buesseler, K. O., Chang, H., Charette, M., Croot, P., Downing, K., Frew, R., Gall, M.,
 415 Hadfield, M., Hall, J., Harvey, M., Jameson, G., LaRoche, J., Liddicoat, M., Ling, R., Maldonado,
 416 M., McKay, R. M., Nodder, S., Pickmere, S., Pridmore, R., Rintoul, S., Safi, K., Sutton, P.,
 417 Strzepek, R., Tanneberger, K., Turner, S., Waite, A., and Zeldis, J.: A mesoscale phytoplankton

- 418 bloom in the polar Southern Ocean stimulated by iron fertilization, *Nature*, 407, 695-702, doi :
419 10.1038/35037500, 2000.
- 420 Boyd, P; W., Jickells, T. D., Law, C. S., Blain, S., Boyle, E. A., Buesseler, K. O., Coale, K. H.,
421 Cullen, J. J., de Baar, H. J. W., Follows, M., Harvey, M., Lancelot, C., Levasseur, M., Owens, N. P.
422 J., Pollard, R., Rivkin, R. B., Sarmiento, J., Schoemann, V., Smetacek, V., Takeda, S., Tsuda, A.,
423 Turner, S., and Watson, A. J.: Mesoscale Iron Enrichment Experiments 1993-2005: Synthesis and
424 Future Directions, *Science*, 315, 612-617, doi: 10.1126/science.1131669, 2007.
- 425 Buck, S. C., Landing, W. M., and Resing, J. A.: Particle size and aerosol iron solubility: A high-
426 resolution analysis of Atlantic aerosols, *Mar. Chem.*, 120, 14-24, doi:
427 10.1016/j.marchem.2008.11.002, 2010a.
- 428 Buck, C. S., Landing, W. M., Resing, J. A., and Measures, C. I.: The solubility and deposition of
429 aerosol Fe and other trace elements in the North Atlantic Ocean: Observations from the A16N
430 CLIVAR/CO₂ repeat hydrography section, *Mar. Chem.*, 120, 57-70, doi:
431 10.1016/j.marchem.2008.08.003, 2010b.
- 432 Caldeira, K., and Duffy, P. B.: The role of the Southern Ocean in uptake and storage of
433 anthropogenic carbon dioxide, *Science*, 287, 620-622,
434 doi : 10.1126/science.287.5453.620, 2000.
- 435 Chen, Y., and Siefert, R. L.: Seasonal and spatial distributions and dry deposition fluxes of
436 atmospheric total and labil iron over the tropical and subtropical North Atlantic Ocean, *J. Geophys.*
437 *Res.*, 109, D09305, doi: 10.1029/2003JD003958, 2004.
- 438 Colin, J.-L., Jaffrezo, J.-L., and Gros, J. M.: Solubility of major species in precipitation: factors of
439 variation, *Atmos. Environ.*, 24A, 537-544, doi: 10.1016/0960-1686(90)90008-B, 1990.
- 440 Desboeufs, K. V., Losno, R., and Colin, J.-L.: Factors influencing aerosol solubility during cloud
441 processes, *Atmos. Environ.*, 35, 3529-3537, [http://dx.doi.org/10.1016/S1352-2310\(00\)00472-6](http://dx.doi.org/10.1016/S1352-2310(00)00472-6),
442 2001.
- 443 Desboeufs, K. V., Sofikitis, A., Losno, R., Colin, J. L., and Ausset, P.: Dissolution and solubility of
444 rare metals from natural and anthropogenic aerosol particulate matter, *Chemosphere*, 58,195-203,
445 doi:10.1016/j.chemosphere.2004.02.025, 2005.
- 446 Draxler, R.R., and Rolph, G.D.: HYSPLIT (HYbrid Single-Particle Lagrangian Integrated
447 Trajectory) Model access via NOAA ARL READY Website

- 448 (<http://ready.arl.noaa.gov/HYSPLIT.php>). NOAA Air Resources Laboratory, Silver Spring, MD,
449 2012.
- 450 Duce, R., and Tindale, N. W.: Chemistry and biology of iron and other trace metals, *Limnol.*
451 *Oceanogr.*, 36(8), 1715-1726, 1991.
- 452 Edwards, R., and Sedwick, P.: Iron in East Antarctic snow: Implications for atmospheric iron
453 deposition and algal production in Antarctic waters, *Geophys. Res. Lett.*, 28, 3907-3910,
454 doi:10.1029/2001GL012867, 2001.
- 455 Feinberg, M.: *Labo-stat – Guide de validation des méthodes d'analyse*, Lavoisier, 361p, 2009.
- 456 Fung, I. Y., Meyn, S. K., Tegen, I., Doney, S. C., John, J. G., and Bishop, J. K. B.: Iron supply and
457 demand in the upper ocean, *Global Biogeochem. Cy.*, 14, 281-295, 2000.
- 458 Gieray, R., Wieser, P., Engelhardt, T., Swietlicki, E., Hansson, H. C., Mentes, B., Orsini, D.,
459 Martinsson, B., Svenningsson, B., Noone, K. J., and Heintzenberg, J.: Phase partitioning of aerosol
460 constituents in cloud [http://dx.doi.org/10.1016/S1352-2310\(96\)00298-1](http://dx.doi.org/10.1016/S1352-2310(96)00298-1) based on single-particle and
461 bulk analysis, *Atmos. Environ.*, 31, 2491-2502, , 1997.
- 462 Guieu, C., Chester, R., Nimmo, M., Martin, J.-M., Guerzoni, S., Nicolas, E., Mateu J., and Keyse,
463 S.: Atmospheric input of dissolved and particulate metals to the northwestern Mediterranean, *Deep-*
464 *Sea Res. II*, 44, 655-674, doi: 10.1016/S0967-0645(97)88508-6, 1997.
- 465 Hand, J.L., Mahowald, N. M., Chen, Y., Siefert, R. L., Luo, C., Bubranianam, A., and Fung, I.:
466 Estimates of atmospheric-processed soluble iron from observations and a global mineral aerosol
467 model: Biogeochemical implications, *J. Geophys. Res.*, 109, D17205, doi: 10.1029/2004JD004575,
468 2004.
- 469 Heimburger, A., Losno, R., Triquet, S., Dulac F., and Mahowald, N. M.: Direct measurements of
470 atmospheric iron, cobalt and aluminium-derived dust deposition at Kerguelen Islands, *Global*
471 *Biogeochem. Cy.*, doi: 10.1029/2012GB004301, 2012a.
- 472 Heimburger, A., Tharaud, M., Monna, F., Losno, R., Desboeufs, K., and Bon Nguyen, E.: SLRS-5
473 Elemental Concentrations of Thirty-Three Uncertified Elements Deduced from SLRS-5/SLRS-4
474 Ratios, *Geostand. Geoanal. Res.*, in press, doi: 10.1111/j.1751-908X.2012.00185.x, 2012b.
- 475 Hsu, S.-C., Wong, G. T. F., Gong, G.-C., Shiah, F.-K., Huang, Y.-T., Kao, S.-J., Tsai, F., Lung, S.-C.
476 C., Lin, F.-J., Lin, I.-I., Hung, C.-C., and Tseng, C.-M.: Sources, solubility, and dry deposition of

- 477 aerosol trace elements over the East China Sea, *Mar. Chem.*, 120, 116-127, doi:
478 10.1016/j.marchem.2008.10.003, 2010.
- 479 Ito, A.: Contrasting the Effect of Iron Mobilization on Soluble Iron Deposition to the Ocean in the
480 Northern and Southern Hemispheres, *Journal of the Meteorological Society of Japan*, 90A, 167-188,
481 doi: 10.2151/jmsj.2012-A09, 2012.
- 482 Jickells, T. D., Davies, T. D., Tranter, M., Landsberger, S., Jarvis, K., and Abrahams, P.: Trace
483 elements in snow samples from Scottish Highlands: sources and dissolved/particulate distributions,
484 *Atmos. Environ.*, 26A, 393-401, doi: 10.1016/0960-1686(92)90325-F, 1992.
- 485 Jickells, T. D., An, Z. S., Andersen, K. K., Baker, A. R., Bergametti, G., Brooks, N., Cao, J. J.,
486 Boyd, P. W., Duce, R. A., Hunter, K. A., Kawahata, H., Kubilay, N., LaRoche, J., Liss, P. S.,
487 Mahowald, N., Prospero, J. M., Ridgwell, A. J., Tegen, I., and Torres, R.: Global Iron Connections
488 Between Desert Dust, Ocean Biogeochemistry, and Climate, *Science*, 308, 67-71, doi:
489 10.1126/science.1105959, 2005.
- 490 Journet, E., Desboeufs, K. V., Caquineau, S., and Colin, J.-L.: Mineralogy as a critical factor of dust
491 iron solubility, *Geophys. Res. Lett.*, 35, L07805, doi: 10/1029/2007/GL031589, 2008.
- 492 Kieber, R. J., Willey, J. D., and Avery Jr., G. B.: Temporal variability of rainwater iron speciation at
493 the Bermuda Atlantic Time Series Station, *J. Geophys. Res.*, 108, n° C8, 3277, doi:
494 10.1029/2001JC001031, 2003.
- 495 Lim, B., Jickells, T. D., Colin, J.-L., and Losno, R.: Solubilities of Al, Pb, Cu, and Zn in rain
496 sampled in the marine environment over the North Atlantic Ocean and Mediterranean Sea, *Global*
497 *Biogeochem. Cy.*, 8, 349-362, doi: 10.1029/94GB01267, 1994.
- 498 Losno, R.: Chimie d'éléments minéraux en trace dans les pluies méditerranéennes, Ph.D. Thesis;
499 Université de Paris 7, 1989.
- 500 Losno, R., Colin, J.-L., Lebris, N., Bergametti, G., Jickells, T., and Lim, B.: Aluminium solubility in
501 rainwater and molten snow, *J. Atmos. Chem.*, 17, 29-43, doi: 10.1007/BF00699112, 1993.
- 502 Mahowald, N. M., Baker, A. R., Bergametti, G., Brooks, N., Duce, R. A., Jickells, T. D., Kubilay,
503 N., Prospero, J. M., and Tegen, I.: Atmospheric global dust cycle and iron inputs to the ocean,
504 *Global Biogeochem. Cy.*, 19, GB4025, doi: 10.1029/2004GB002402, 2005.
- 505 Mahowald, N. M.: Anthropocene changes in desert area: Sensitivity to climate model predictions,

- 506 Geophys. Res. Lett., 34, L18817, doi:10.1029/2007GL030472, 2007.
- 507 Martin, J. H.: The iron hypothesis, *Paleoceanography* 5, 1-13, 1990.
- 508 Middag, R., de Baar, H. J. W., Laan, P., Cai, P. H., van Ooijen, J. C.: Dissolved manganese in the
509 Atlantic sector of the Southern Ocean, *Deep-Sea Res. II*, 58, 2661-2677, doi:
510 10.1016/j.drs2.2010.10.043, 2011.
- 511 Morel, F. M., Hudson, R. J. M., and Price, N. M.: Limitation of productivity by trace metals in the
512 sea, *Limnol. Oceanogr.*, 36(8), 1742-1755, doi: 10.4319/lo.1991.36.8.1742, 1991.
- 513 Morel, F. M. M., and Price, N. M.: The Biogeochemical Cycles of Trace Metals in the Oceans,
514 *Science*, 300, 944-948, doi: 10.1126/science.1083545, 2003.
- 515 Paris, R., Desboeufs, K. V., Formenti, P., Nava, S., and Chou, C.: Chemical characterisation of iron
516 in dust and biomass burning aerosols during AMMA-SOP0/DABEX: implication for iron solubility,
517 *Atmos. Chem. Phys.*, 10, 4273-4282, doi:10.5194/acp-10-4273-2010, 2010.
- 518 Paris, R., Desboeufs, K. V., and Journet, E.: Variability of dust iron solubility in atmospheric waters:
519 investigation of the role of oxalate organic complexation, *Atmos. Chem. Phys.*, 45, 5510-5517, doi:
520 10.1016/j.atmosenv.2011.08.068, 2011.
- 521 Price, N. M., and Morel, F. M. M.: Colimitation of phytoplankton growth by nickel and nitrogen,
522 *Limnol. Oceanogr.*, 36(6), 1071-1077, doi: 10.4319/lo.1991.36.6.1071, 1991.
- 523 Prospero, J.M., Ginoux, P., Torres, O., Nicholson, S.E., and Gill, T.E.: Environmental
524 characterization of global sources of atmospheric soil dust identified with the NIMBUS 7 TOMS
525 absorbing aerosol product, *Rev. Geophys.*, 40, doi: 10.1029/2000RG000095, 2002.
- 526 Pruppacher, H.R., and Jaenicke, R.: Processing of water-vapor and aerosols by atmospheric clouds,
527 a global estimate, *Atmos. Res.*, 38, 283-295, [http://dx.doi.org/10.1016/0169-8095\(94\)00098-X](http://dx.doi.org/10.1016/0169-8095(94)00098-X),
528 1995.
- 529 Rolph, G.D.: Real-time Environmental Applications and Display sYstem (READY) Website
530 (<http://ready.arl.noaa.gov>). NOAA Air Resources Laboratory, Silver Spring, MD, 2012.
- 531 Saito, M.A., Moffett, J.W., Chisholm, S.W., and Waterbury, J.B.: Cobalt limitation and uptake in
532 *Prochlorococcus*, *Limnol. Oceanogr.*, 47, 1629–1636, doi: 10.4319/lo.2002.47.6.1629, 2002.
- 533 Sarmiento, J. L., Hughes, T. M. C., Stouffer, R. J., and Manabe, S.: Simulated response of the ocean
534 carbon cycle to anthropogenic climate warming, *Nature*, 393, doi:10.1038/30455, 1998.

- 535 Schlitzer, R.: Applying Adjoint Method for Biogeochemical Modeling: Export of Particulate
536 Organic Matter in the World Ocean, *Geoph. Monog. Series.*, 107-124, 2000.
- 537 Shi, Z., Krom, M. D., Jickells, T. D., Bonneville, S., Carslaw, K. S., Mihalopoulos, N., Baker, A. R.,
538 Benning, L. G.: Impacts on iron solubility in the mineral dust by processes in the source region and
539 the atmosphere: A review, *Aeolian Res.*, 5, 21-42, doi: 10.1016/j.aeolia.2012.03.001, 2012.
- 540 Siefert, R. L., Johansen, A. M., and Hoffmann, M. R.: Chemical characterization of ambient aerosol
541 collected during the south-west monsoon and inter-monsoon seasons over the Arabian Sea: Labile-
542 Fe(II) and other trace metals, *J. Geophys. Res.*, 104, 3511 – 3526, doi: 10.1029/1998JD100067,
543 1999.
- 544 Theodosi, C., Markaki, Z., Tselepidis, A., and Mihalopoulos, N.: The significance of atmospheric
545 inputs of soluble and particulate major and trace metals to the eastern Mediterranean seawater, *Mar.*
546 *Chem.*, 120, 154-163, doi: 10.1016/j.marchem.2010.02.003, 2010.
- 547 Wagener, T., Guieu, C., Losno, R., Bonnet, S., and Mahowald, N.: Revisiting atmospheric dust
548 export to the Southern Hemisphere ocean: Biogeochemical implications, *Global Biogeochem. Cy.*,
549 22, GB2006, doi: 10.1029/2007GB002984, 2008.
- 550 Witt, M.L.I., Mather, T. A., Baker, A. R., De Hoog, J. C. M., and Pyle, D.M.: Atmospheric trace
551 metals over the south-west Indian Ocean: Total gaseous mercury, aerosol trace metal concentrations
552 and lead isotope ratios, *Mar. Chem.*, 121, 2-16, doi: 10.1016/j.marchem.2010.02.005, 2010.
- 553 Zhuang, G., Yi, Z., Duce, R. A., and Brown, P. R. : Chemistry of iron in Marine aerosols, *Global*
554 *Biogeochem. Cy.*, 6, 161-173, doi: 10.1029/92GB00756, 1992.

555

556

557 **Tables:**

558 Table 1:

559 Detection limits, accuracy and reproducibility of SLRS-5 measurements, estimated recovery rate of
 560 BE-N and SDC-1.

Element	m/z (res.)	DL (ng/L)	SLRS-5			BEN	SDC-1
			measured values $\pm \sigma$ ($\mu\text{g/L}$)	RSD%	RR%	RR %	RR %
Al	27 (m)	26.4	51 \pm 3	6%	102%	112%	74%
Ce	140 (l)	0.036	0.257 \pm 0.014	5%	109%	121%	
Fe	56 (m)	5.2	93.0 \pm 4.6	5%	102%	129%	105%
La	139 (l)	0.039	0.199 \pm 0.011	5%	101%	111%	
Mn	55 (m)	0.62	4.50 \pm 0.20	5%	104%	143%	111%
561 Nd	146 (l)	0.11	0.183 \pm 0.008	4%	99%	112%	
Ti	47 (m)	1.7	2.14 \pm 0.22	10%	94%	151%	109%

562 m/z = mass of the considered isotope; res.= resolution; h = high resolution ($> 10,000$) , m =
 563 medium resolution ($\approx 4,000$) , l = low resolution (≈ 300); DL = detection limit; RSD% =
 564 reproducibility, RR% = recovery rate.

565

566

567 **Table 2**568 **Sampling conditions for the discussed rain events. The funnel collecting surface is 0.045 m².**

Sample name	Sampling period	Collected volume	Wind direction
P3_08	7/12/2008 from 8:30 to 11:55	0.320 L	W-SW
P6_08	from 10/12/2008 (22:30) to 11/12/2008 (19:00)	0.101 L	W-NW
P3_09	11/12/2009 from 8:05 to 17:30	0.029 L	W-SW
P1_10	from 24/11/2010 (19:00) to 25/11/2010 (9:00)	0.536 L	W-NW
P3_10	30/11/2010 from 15:50 to 22:30	0.453 L	N-NW

569

25

570 **Table 3:**

571 **Rain event fluxes ($\mu\text{g m}^{-2}$) \pm uncertainties**

	P3_08	P6_08	P3_09	P1_10	P3_10
Al	32 \pm 5	11 \pm 3	12 \pm 3	12 \pm 3	52 \pm 7
Ce	0.048 \pm 0.010	0.021 \pm 0.005	0.021 \pm 0.004	0.024 \pm 0.005	0.11 \pm 0.02
Fe	13 \pm 3	8.3 \pm 3.2	7.5 \pm 3.4	8.5 \pm 3.4	31 \pm 4
La	0.025 \pm 0.003	0.011 \pm 0.001	0.0090 \pm 0.0009	0.011 \pm 0.001	0.041 \pm 0.004
Mn	0.34 \pm 0.06	0.23 \pm 0.05	0.21 \pm 0.06	0.82 \pm 0.11	1.29 \pm 0.16
Nd	0.018 \pm 0.002	0.0079 \pm 0.0008	0.0075 \pm 0.0008	0.0069 \pm 0.0015	0.043 \pm 0.004
Ti	2.2 \pm 0.8	1.0 \pm 0.5	1.1 \pm 0.7	0.82 \pm 0.65	2.4 \pm 0.8

573 **Uncertainties are computed by propagating standard deviations of Eq. 5 and Eq. 6.**

574

575

576 **Table 4:**577 **Solubility (%) in rainwater.**

	P3_08	P6_08	P3_09	P1_10	P3_10
Al	92% ± 2%	95% ± 3%	67% ± 9%	70% ± 8%	96% ± 1%
Ce	94% ± 1%	92% ± 2%	68% ± 7%	84% ± 3%	96% ± 1%
Fe	82% ± 5%	85% ± 5%	51% ± 22%	57% ± 17%	91% ± 2%
La	95% ± 1%	96% ± 1%	70% ± 4%	83% ± 2%	96% ± 1%
Mn	88% ± 4%	89% ± 4%	66% ± 11%	89% ± 3%	94% ± 2%
578 Nd	95% ± 1%	98% ± 2%	70% ± 4%	79% ± 4%	96% ± 1%
Ti	76% ± 14%	83% ± 21%	46% ± 32%	33% ± 44%	79% ± 13%

579 **Absolute uncertainties (±) are computed using Eq. 7 for each rain sample.**

580 Figure captions:

581 Figure 1:

582 a) Kerguelen Islands in the Southern Indian Ocean.

583 b) *Port-aux-Français* on Kerguelen Islands plus picture of rainwater sampling device on PAF.

584

585 Figure 2: (a) Rainwater sampling device on the top of its PVC tube, (b) drawing of the sampling
586 device, the sampling funnel is cut here.

587

588 Figure 3: Ratio of the median quantities in blanks (all the blanks pooled together) relative to both
589 median soluble (grey) and median insoluble (black) quantities in rainwater samples for all the
590 measured elements.

591

592 Figure 4: Ti/Al ratios in rainwater samples (grey histogram), in soil samples (dotted black line +
593 hatched rectangle for uncertainties; Heimburger et al., 2012a) and in deposition samples (black line;
594 Heimburger et al., 2012a). Ti/Al in P3_10, P1_10, P3_08, P6_08 and P3_09 exhibit values not
595 compatible with the range of Ti/Al found in soil collected on Kerguelen Islands; these five rains
596 were then considered as not significantly influenced by local soil contamination and so
597 representative of long range transport particles.

598

599

600

601

602

603

604

605

606

28

607

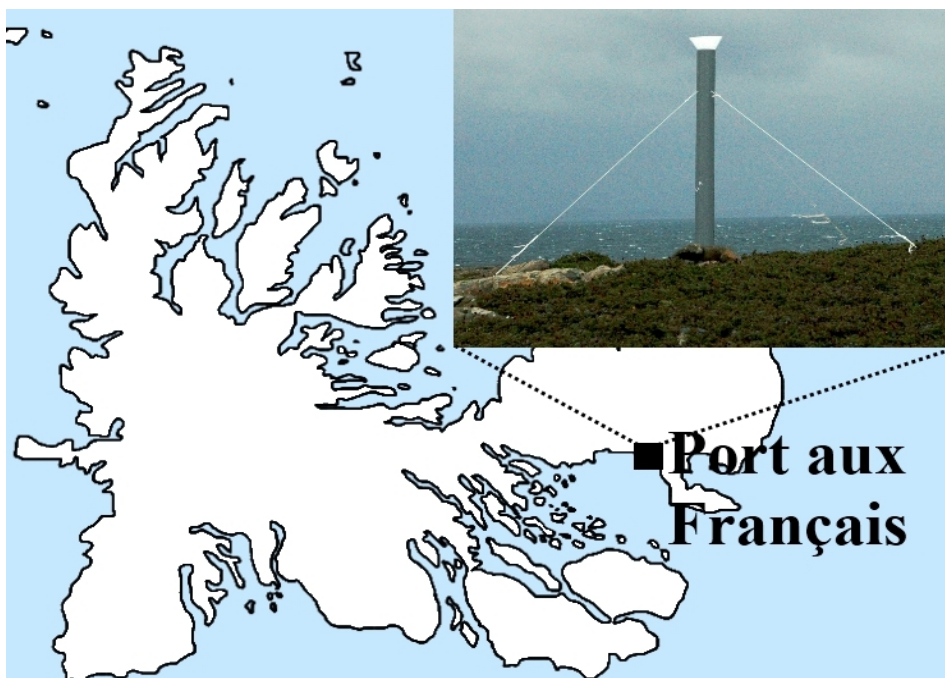
608 Figure 1:

609 a) Kerguelen Islands in the Southern Indian Ocean.



610

611 b) *Port-aux-Français* on Kerguelen Islands plus picture of rainwater sampling device on PAF.



612

613 Credit: authors

614 Figure 2:

615 (a) Rainwater sampling device on the top of its PVC tube



616

617 Credit: authors.

618

619

620

621

622

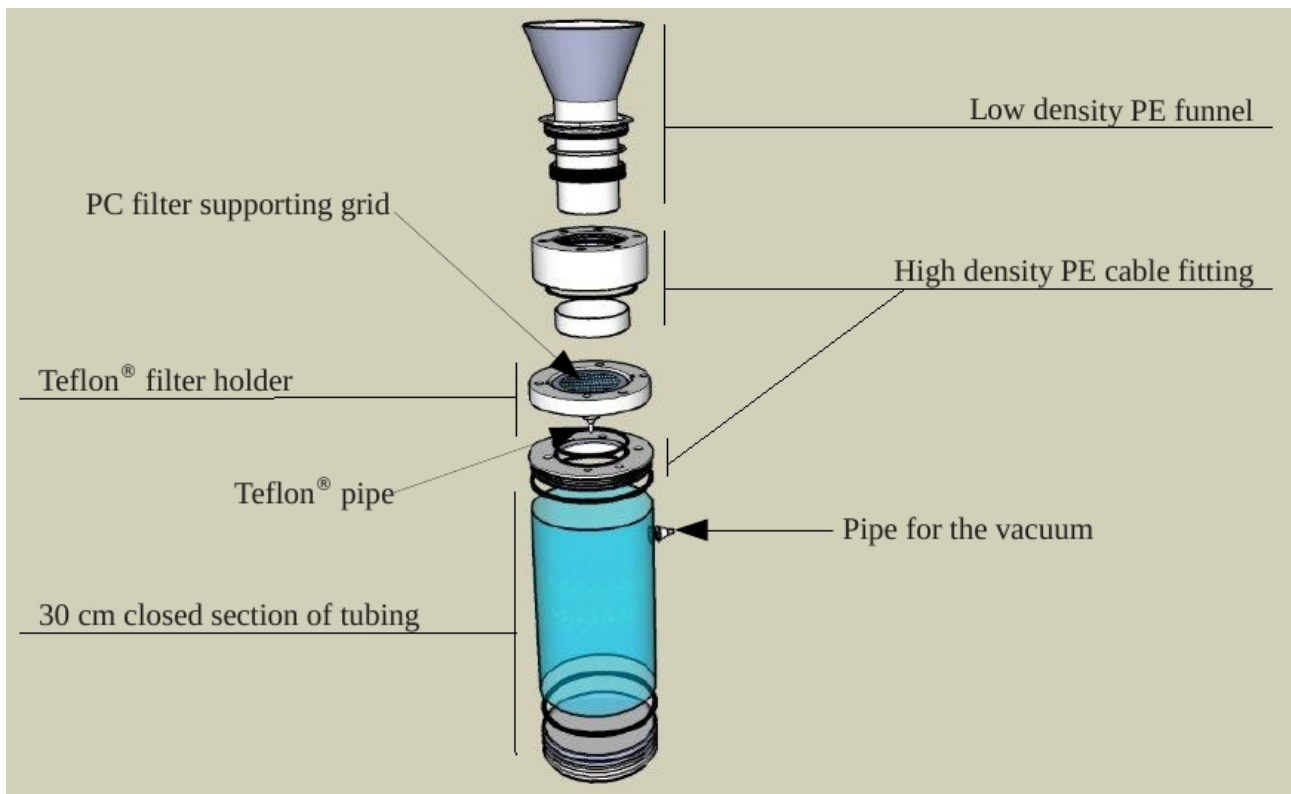
623

624

625

30

626 (b) Drawing of the sampling device, the sampling funnel is cut here.

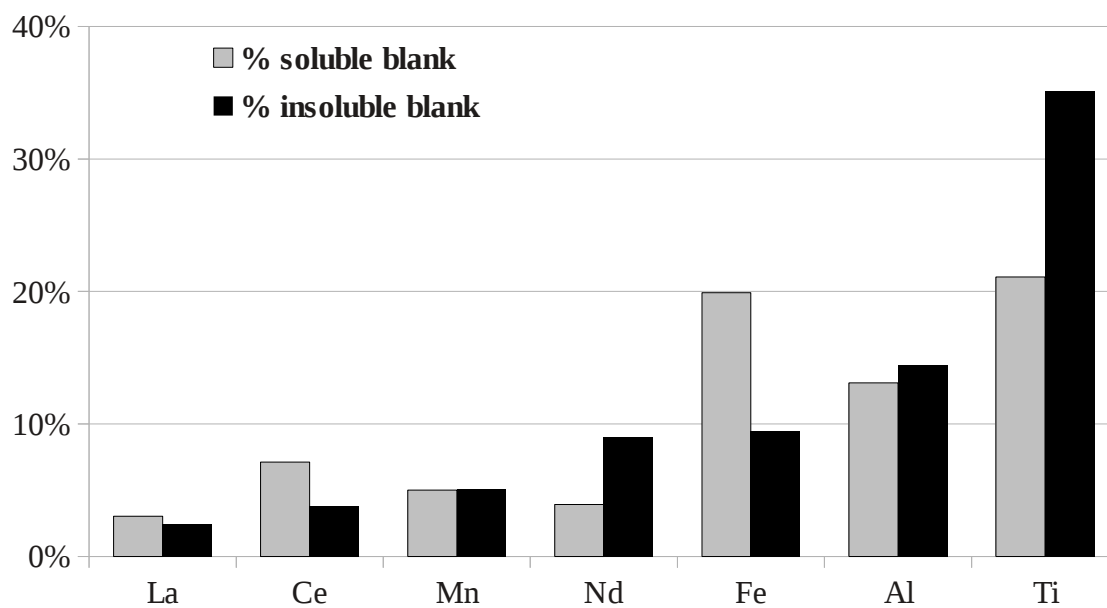


627

628

629 Figure 3:

630 Ratio of the median quantities in blanks (all the blanks pooled together) relative to both median
631 soluble (grey) and median insoluble (black) quantities in rainwater samples for all the measured
632 elements.



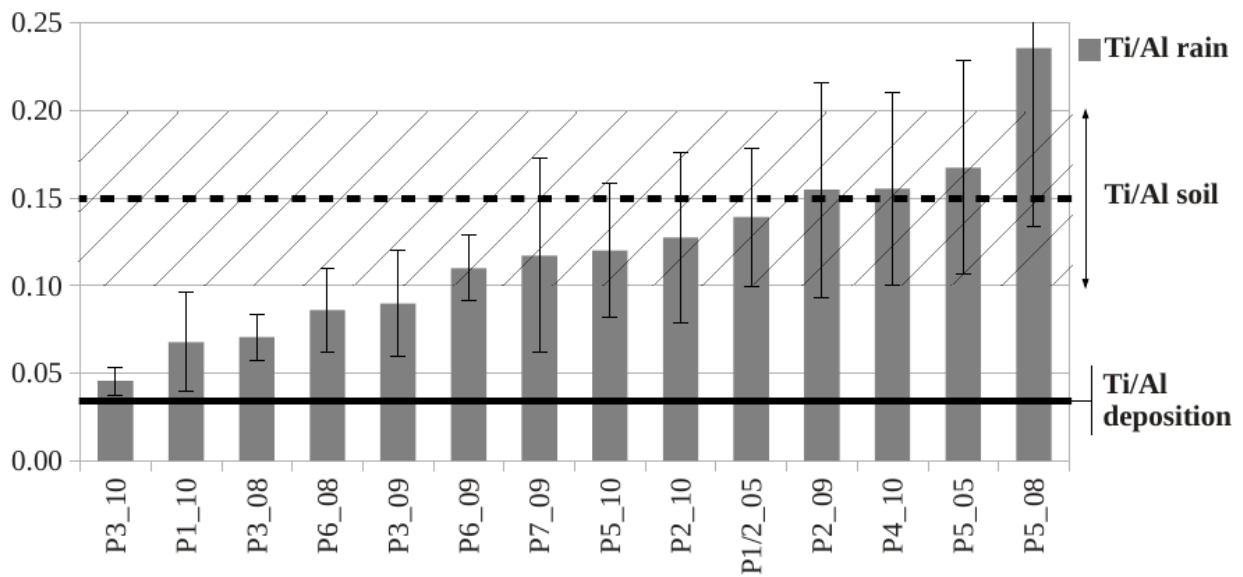
633

634

635

636 **Figure 4:**

637 **Ti/Al ratios in rainwater samples (grey histogram), in soil samples (dotted black line + hatched**
638 **rectangle for uncertainties; Heimburger et al., 2012a) and in deposition samples (black line;**
639 **Heimburger et al., 2012a). Ti/Al in P3_10, P1_10, P3_08, P6_08 and P3_09 exhibit values not**
640 **compatible with the range of Ti/Al found in soil collected on Kerguelen Islands; these five rains**
641 **were then considered as not significantly influenced by local soil contamination and so**
642 **representative of long range transport.**



643

644

645